PHILOSOPHICAL TRANSACTIONS OF THE ROYAL SOCIETY A MATHEMATICAL, PHYSICAL & ENGINEERING SCIENCES

The Stability of Fission Products in Uranium Dioxide

R. W. Grimes and C. R. A. Catlow

Phil. Trans. R. Soc. Lond. A 1991 **335**, 609-634
doi: 10.1098/rsta.1991.0062

The stability of fission products in uranium dioxide

By R. W. Grimes and C. R. A. Catlow

Davy Faraday Research Laboratory, The Royal Institution of Great Britain, 21 Albemarle Street, London W1X 4BS, U.K.

A review of experimental data concerning the behaviour of fission products in nuclear fuels is used to illustrate the significant variation in solubility exhibited by the different species. To understand the reasons for this variation, it is necessary to obtain a reliable estimate of the solution energies and thus to determine the most stable solution site. This we suggest will be critical in predicting the behaviour of nuclear fuels in both accident and normal operating conditions. We have therefore used the Mott–Littleton simulation technique to calculate solution energies for the fission products Br, Kr, Rb, Sr, Y, Zr, Te, I, Xe, Cs, Ba, La and Ce in UO_2. We considered solution at both uranium and oxygen vacancies, the interstitial site and at the di-, tri- and tetra-vacancy complexes. Non-stoichiometry and variable charge state are important components of the model.

From these results we conclude that the solubility is significantly affected by non-stoichiometry. In UO_2 and UO_{2-x}, products such as Cs, Rb and Ba are thermodynamically more stable as binary oxide precipitates. Conversely, Y, La and Sr are soluble in UO_2 and UO_{2+x}, while Cs, Rb, Sr and Ba are only soluble in UO_{2+x}. The behaviour of I, Br and Te is complicated by the fact that these species are most stable as anions in UO_2 and UO_{2-x} but as cations in UO_{2+x}. In our model, Zr and the inert gas species Xe and Kr are always predicted to be insoluble, while CeO_2 will form a solid solution with UO_2.

1. Introduction

(a) *Fission product formation*

The majority of power generating nuclear fuels are constructed from pellets of polycrystalline UO_2 or UO_2–PuO_2 solid solutions. The pellets are assembled into long rods which are sealed (or clad) inside a helium-filled gas tight canister. Fuels may be classified in terms of the percentage of actinide ions that undergo fission (burn-up) during the useful lifetime of the fuel. In conventional water and gas cooled reactors, burn-up will typically reach a maximum of 4% while in sodium cooled fast breeder reactors this figure is closer to 12%. Fuels presently being developed should achieve burn-ups close to 20% (Gittus *et al.* 1989). Conventional and fast reactor fuels also operate at different temperatures. The centre of fuel in a conventional reactor will operate at 1500 K while fast reactor fuel will reach higher temperatures, usually around 2300 K. In both cases, the periphery of the fuel assembly is at a lower temperature resulting in a temperature gradient across the fuel.

Fission of so many atoms causes the formation of significant numbers of decay products. Figure 1 shows the yield of fission products calculated using the FISPIN code for a 3.2% enriched PWR fuel pin rated at 45 kW m^{-1} after 2.9% burn-up (R. G. J. Ball, personal communication). The y-coordinate expresses the number of

Phil. Trans. R. Soc. Lond. A (1991) **335**, 609–634
Printed in Great Britain

atoms of a particular fission product produced through the fission of 100 uranium atoms. Although the absolute values presented in figure 1 are specific to a particular fuel pin, they reproduce the general trends found in other studies (see, for example, Ewart *et al.* 1976; Kleykamp 1985; Imoto 1986; Kleykamp 1990). In this example, a 2.9% burn-up of the total actinide inventory implies that 3.5 atoms of uranium out of every 100 have been lost and 0.6 atoms of Pu have been formed. This degree of cation loss is easily accommodated by the UO_2 lattice which at 1500 K may exhibit a non-stoichiometry equivalent to a loss of over 10% of its cations (Kovba 1970; Latta & Fryxell 1970). Indeed, the stability of UO_2 over this wide range of non-stoichiometry is one of the reasons it is so useful as a nuclear fuel.

Although fuel burn-up creates many new nuclei, the average valence of fission products is significantly less than four (Davies & Ewart 1971; Ewart *et al.* 1976). This causes the fuel to become more oxidized which, since external oxygen is not available, results in the formation of U^{5+} ions. For the PWR pin described in figure 1, the average charge of the uranium ions is estimated to be 4.01. This value assumes that fission products form oxides, metal precipitates or gas phase molecules as outlined in table 1.

Since fission products differ in their physical and chemical interactions with the fuel matrix and fuel assembly, the relative importance of a fission product cannot be considered on the basis of yield alone. There have been a number of attempts to classify fission products into chemical groups (see, for example, Kleykamp 1985; Imoto 1986; Gittus *et al.* 1989). These are summarized in table 1 and a more detailed discussion is presented below. In all cases, the actual distribution of precipitates is largely governed by the thermal gradient across the fuel (Ewart *et al.* 1976; Nichols 1979; Kleykamp 1985).

(*b*) *Fission product behaviour*

(i) *Volatile products*

The inert gas atoms Xe and Kr are known to be insoluble in the UO_2 matrix. They are only found in the fuel as a consequence of fission. Thus, at sufficiently high temperatures, gas atoms may migrate (possibly via radiation-induced re-solution (Turnbull & Cornell 1971)) to grain boundaries, dislocation loops or pre-existing pores where they aggregate into bubbles (Matzke & Davies 1967; Matzke 1980) or vent to the fuel-clad gap. Bubble formation is important since it degrades mechanical properties, leads to fuel swelling and as such must be considered as a performance limiting factor. In addition, recent work by MacInnes & Winter (1987) suggests that Xe and Kr although chemically inert will reduce the oxygen potential of UO_2 since oxygen ions will bind to defect clusters in which fission gas is trapped. An interesting recent observation (Thomas & Guenther 1989) suggests that the Xe trapped in bubbles can be at high enough pressures for the inert gas to form a solid. Similar results have been noted for high pressure Xe bubbles in metals (Templier *et al.* 1986).

At the atomic level, channelling experiments carried out on UO_2 single crystals containing ^{222}Rn showed that the radon did not occupy a normal lattice site (Matzke & Davies 1967). By inference, it was suggested that xenon would also not occupy a lattice site. This assumption is supported by the observation that xenon diffusion in UO_2 is unaffected by doping with either penta- or tri-valent ions. Such a result is consistent with xenon diffusion via neutral tri-vacancy clusters (Matzke 1980).

Iodine and bromine are also volatile fission products and a significant fraction of their yield can be released to the fuel-clad gap. However, unlike the inert gas species,

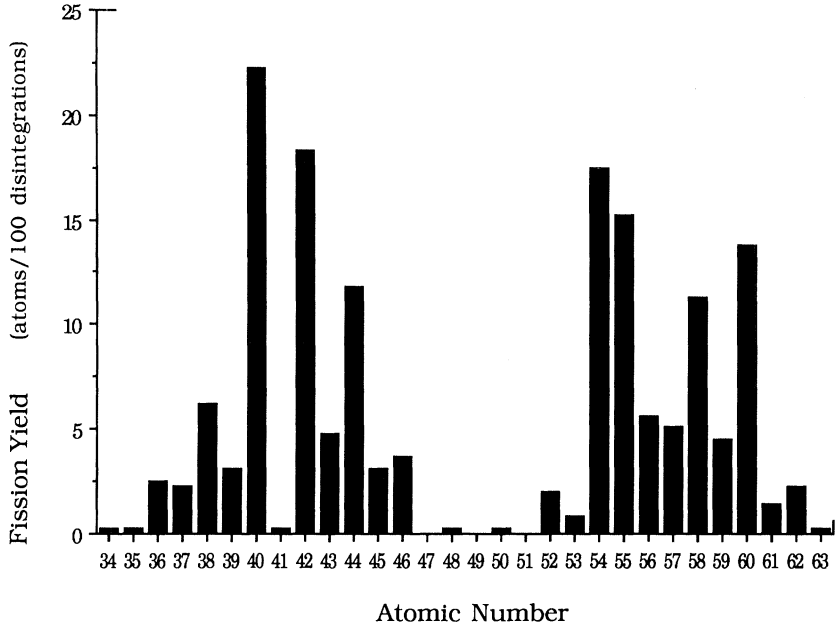

Figure 1. Fission yield for a PWR fuel rod after 2.9% burn-up.

Table 1. *Chemical state of fission products in irradiated fuel*

fission products[a]	likely chemical state	% of fission yield[b]
Xe, Kr, Br, I (Cs, Rb, Te)	volatile product	13+(12)
Cs, Rb, Ba, Zr, Nb, Te (Mo, Sr)	oxide precipitate	30+(15)
Mo, Tc, Ru, Rh, Pd, Ag, Cd, In, Sn, Sb (Te)	metallic precipitate	27+(1)
Sr, Y, La, Ce, Pr, Nd, Pm, Sm, Nb (Zr, Ba, Te)	products in solid solution	30+(19)

[a] Brackets indicate elements that exhibit the possibility of an alternative chemical state.
[b] For a 3.2% enriched PWR fuel rod at 2.9% burn-up. The bracketed figures correspond to the bracketed elements in column 1.

the halide ions are chemically active and may react with other species in the fuel-clad gap (Ball *et al.* 1989). Indeed, it has been suggested that iodine may be important chemically as it can react with the zircalloy fuel-cladding material of a PWR reactor and cause stress corrosion cracking (see, for example, Yang & Tsai 1989; Schuster & Lemaignan 1989). However, recent calculations (Ball *et al.* 1989) suggest that under normal operating conditions, the amount of iodine in the fuel-clad gap will always be less than the critical concentration necessary to cause stress corrosion cracking. Nevertheless, and despite its small fission yield (see figure 1), the need to limit the concentration of iodine in the fuel-clad gap must be an important consideration in reactor design (Gittus *et al.* 1989).

Kleykamp (1985) has suggested that some iodine might react with other fission products, notably caesium and become trapped within the fuel. However, this suggestion seems unlikely since iodine migrates much faster than caesium (Prussin *et al.* 1988) and profiling experiments have shown that iodine and caesium concentrate at different places in the fuel (Kleykamp 1985).

PHILOSOPHICAL TRANSACTIONS OF THE ROYAL SOCIETY A MATHEMATICAL, PHYSICAL & ENGINEERING SCIENCES

(ii) *Oxide precipitates*

A number of fission products precipitate out of solution in the form of complex oxides. These are known collectively as the grey phase (Kleykamp *et al.* 1985). Although the composition of grey phase precipitates will vary with fuel composition and reactor history, the main constituents are Ba, Zr, U and Pu with smaller amounts of Sr, Mo, Te, Cs, Rb and the lanthanide ions. The most commonly reported precipitates are the perovskite oxides $[Ba_{1-x-y}Sr_xCs_y](U, Pu, Ln, Zr, Mo)O_3$ which are essentially substituted $BaZrO_3$. Sari *et al.* (1979) identified an example of these, $(Ba_{0.90}Sr_{0.05}Cs_{0.05})[Zr_{0.54}Mo_{0.14}U_{0.18}Pu_{0.14}]O_3$, in mixed oxide fuel after 6% burn-up. However, simpler rock-salt type oxides such as $Ba_xSr_{1-x}O$ have also been observed (Kleykamp *et al.* 1985). It is important to note that grey phase precipitates were not detected in transition electron microscopy studies of low operating temperature light water reactor (LWR) fuels (Thomas & Guenther 1989). However, grey phase precipitates are known to form in LWR fuels that have been subjected to higher than normal operating temperatures (I. Ray, personal communication 1990).

Despite their large fission yield, Cs and Rb are only minor components of the grey phase. This is due primarily to their relatively volatile nature, although with increasing oxygen potential, Cs is known to react with UO_2 to form Cs_2UO_4 (Fee & Johnson 1978; Une 1985). As with other volatile products, Cs and Rb form bubbles of the sort generally associated with Xe and Kr (Matzke 1989). Subsequently, Cs and Rb diffuse to the fuel-clad gap where they may react with volatile I and Br. Alternatively, at high oxygen pressures, Cs is known to corrode cladding materials such as zircalloy (Kleykamp 1979, 1990) possibly forming Cs_2ZrO_3 (Gittus *et al.* 1989). Caesium will also react with stainless steel (Walker 1978) to form Cs_3CrO_4 (Fee *et al.* 1979). The latter is of particular concern because in combination with Te, Cs is known to promote stress corrosion cracking in stainless steel (Adamson *et al.* 1982). We should note that even in the absence of Cs, Te will corrode stainless steel (Pulham & Richards 1990).

Although Cs is largely insoluble in UO_2 (Kleykamp 1985), it has been noted that the retained fraction is greatest in fuels with a higher oxygen to metal ratio (Phillips *et al.* 1974). For such ions, implantation studies reveal that both Cs and Rb occupy lattice sites (Matzke & Blank 1989). This observation is important to the present work as it provides information concerning the most stable solution site in UO_2 even though solution is not thermodynamically preferred.

The behaviour of tellurium is complex and with only a small fission yield, it is usually difficult to detect. However, tellurium is known to combine with fission products such as Cs, Sn, Pd, U and Pu to form metallic inclusions located both in the fuel and near the fuel–clad interface (Ewart *et al.* 1976). In addition, tellurium can precipitate out of solution in complex oxide phases such as $(Ba_{1-x}Sr_x)TeO_3$ (Pearce *et al.* 1983; Kleykamp 1985). Finally, since tellurium has an appreciable solubility in UO_2, a significant proportion is expected to remain in the fuel (Kleykamp 1985). Recent ion implantation experiments (Matzke & Blank 1989) suggest that in solution, Te occupies a lattice site. The equilibrium between different tellurium containing phases and its dependence on oxygen partial pressure is not well characterized.

PHILOSOPHICAL TRANSACTIONS OF THE ROYAL SOCIETY A MATHEMATICAL, PHYSICAL & ENGINEERING SCIENCES

(iii) *Products in solid solution*

The fission products Sr, Y, Nb and the lanthanide ions are generally regarded as soluble in UO_2. Lanthanide ions, in particular, form fluorite structured solid solutions with UO_2 over a sufficiently large range of both composition and stoichiometry to encompass any situations that might result from even very high levels of fuel burn-up (DeAlleluia *et al.* 1981).

Unlike the case for lanthanide ions, the extent of Sr solubility depends critically upon the oxygen to metal ratio. For example, Kleykamp (1985), states that the solubility of Sr is over ten times higher in UO_2 than it is in $UO_{1.94}$. Insoluble Sr precipitates out of solution in a barium containing grey oxide phase. Barium, which is of course chemically similar to Sr, is known to exhibit only a limited solubility; an example in $U_{0.8}Pu_{0.2}O_2$ has been reported by Sari *et al.* (1979). Calculations using the SOLGASMIX code (which is based on thermodynamic data and minimizes the total Gibbs energy for an ensemble of phases (Imoto 1986)) also predict that Sr is significantly more soluble in UO_2 than Ba. Thus, in most fuels (as in the results of Maeda *et al.* (1984) in simulated high burn-up mixed oxide) it appears that Sr will be contained in the fuel while Ba will be observed in precipitates of typically $BaZrO_3$ or BaO.

Different solubilities are also observed for Ce and Zr; in this case, Ce is more soluble than Zr (Markin *et al.* 1970; Romberger *et al.* 1967). In fact, concentrations of CeO_2 in excess of anything that will be formed through fission exhibit complete solid solubility in UO_2 over its entire range of non-stoichiometry even at room temperature (Markin *et al.* 1970). Conversely, ZrO_2 in excess of 0.4 mole% (which should be formed at less than 1% burn-up) is only soluble above 1350 °C (Romberger *et al.* 1967). This temperature is above that of fuel in conventional reactors but below the operating temperature of a fast breeder reactor.

(iv) *Metallic precipitates*

Approximately one quarter of the fission product inventory will precipitate out of solution to form a dispersion of metallic inclusions (Ewart *et al.* 1976; Kleykamp *et al.* 1985; Thomas *et al.* 1989). The precipitates, known collectively as the white or ϵ-ruthenium phase are composed mainly of the 4d transition metal ions Mo, Tc, Ru, Rh and Pd and are formed in both LWR and high temperature fuels. The exact composition of the particles depends upon the original fuel composition, burn-up and thermal gradient but most precipitates exhibit a hexagonal structure characteristic of an alloy between the two largest fission yield elements in this group, Mo and Ru. The ratio of Mo to Ru is controlled by the oxygen potential of the fuel. As burn-up proceeds and more oxygen becomes available, the Mo is oxidized to MoO_2 which is insoluble in the fuel but is available for incorporation in grey phase precipitates (Kleykamp 1985). Conversely, Tc, Ru, Rh and Pd are much harder to oxidize and remain in the metallic precipitates (Ewart *et al.* 1976). This leads to a wide range of possible compositions for the white (metallic) and grey (oxide) phases at different fuel burn-ups.

(*c*) *Materials implications*

In our discussion of the behaviour of fission products in nuclear fuels we have attempted to draw attention to the major materials problems that must be understood at a microscopic level in order that the behaviour of the fuel can be predicted at a macroscopic level. It is also important to provide information pertinent to both

PHILOSOPHICAL TRANSACTIONS OF THE ROYAL SOCIETY A MATHEMATICAL, PHYSICAL & ENGINEERING SCIENCES

accident (Cubicciotti 1988; Ball *et al.* 1989) and normal operating conditions. In both cases, fuel behaviour will be intimately connected with changes in the stoichiometry and the concentration of fission products. In the case of normal operating conditions, stoichiometry and fission product concentrations are connected since we expect fuel to become more hyper-stoichiometric as actinide burn-up continues. During accidents such as a breach of the cladding material, fuel may be subjected to very oxidizing conditions as is the case in a water-cooled reactor or to very reducing atmospheres if the reactor is cooled by sodium. Since in one case a breach of the cladding causes the fuel to become hyper-stoichiometric and in the other to become hypo-stoichiometric the repercussions on fission product stability will be quite different.

A considerable improvement in the understanding and prediction of the equilibria between fission products and the fuel matrix could be gained by a determination of the site stability and solubility of the fission products. Since experiments are extremely difficult and expensive, reliable calculations are of particular value. This has provided the impetus to develop a theoretical model by which it is possible to study the energetics of a range of oxide and gas phase fission products under differing fuel conditions. The approximations inherent in our model render it most appropriate for ionic and semi-ionic systems. Thus, calculations involving the metallic precipitates are outside the scope of our study.

2. UO_2: Crystal structure; defects and non-stoichiometry

UO_2 adopts the fluorite structure: the uranium 4+ ions are therefore in the centre of a cube of oxygen ions while the oxygen 2− ions are tetrahedrally coordinated by uranium (see figure 2). Interstitial ions may be accommodated at vacant cube centre sites as shown in figure 3. The intrinsic defect structure of UO_2 is dominated by anion Frenkel disorder with Frenkel pair formation energies in the range of 4–5 eV (Jackson *et al.* 1986; Matzke 1987). Schottky trio energies are higher (8–10 eV) while cation Frenkel energies are sufficiently high for these defects to be of negligible importance. The mobility of cationic defects is low with vacancy migration energies of more than 2 eV. Activation energies for oxygen defects are much lower; *ca.* 1 eV for oxygen interstitials and *ca.* 0.5 eV for oxygen vacancies. The much greater mobility of oxygen compared with uranium has important consequences for the behaviour of the material.

A key feature of the solid state chemistry of UO_2 is the extensive deviations that may occur from the stoichiometric composition. In hyper-stoichiometric UO_{2+x}, at elevated temperatures, x may attain a value of 0.25 with a maximum possible deviation at 1400 K (a typical operating temperature for a conventional reactor) of 0.22 (Kovba 1970). For hypo-stoichiometric UO_{2-x}, lower deviations from stoichiometry are observed with x reaching a maximum value of only 0.02 at 1800 K, although this may increase to 0.30 by 2800 K (Latta & Fryxell 1970). In the non-stoichiometric phases, the defect structure is dominated by the oxygen defects that are created as a consequence of the oxygen excess or deficiency, i.e. oxygen interstitials in UO_{2+x} and vacancies in UO_{2-x}. Indeed, the intrinsic defects will control the defect structure for all values of x such that $|x| < (K_f)^{\frac{1}{2}}$, where K_f is the Frenkel defect equilibrium constant.

Although oxygen vacancies and interstitials are the majority defects in UO_2, minority defects can play a dominant role in fission-product–lattice interactions if

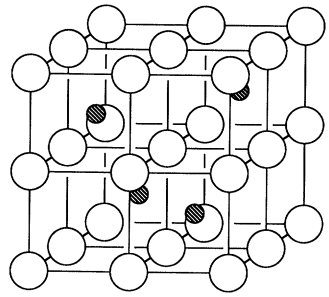

Figure 2. The fluorite lattice. The large unfilled circles represent O^{2-} ions. The smaller hatched circles are U^{4+} ions. Every other cube centre is occupied by a U^{4+} ion.

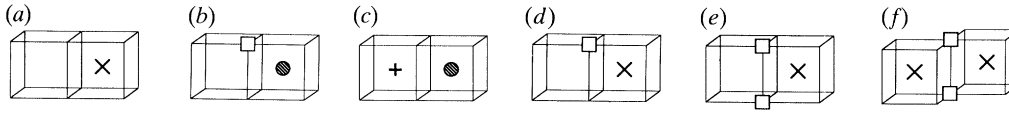

Figure 3. Solution sites for fission products and the solution site effective charge. □, Oxygen vacancy; ●, uranium ion; ×, uranium vacancy; +, interstitial site. (*a*) Uranium vacancy (4−); (*b*) oxygen vacancy (2+); (*c*) interstitial site (0); (*d*) di-vacancy (2−); (*e*) tri-vacancy (2−); (*f*) tetra-vacancy (4−).

fission product solubility is much greater at the minority defect site. Such processes are encouraged by the continuous formation of thermodynamically less favourable defects through radiation damage and high-temperature effects. The defects and defect clusters we shall consider in this study are shown in figure 3; these solution sites provide the range in size and effective charge necessary to accommodate the variety of fission products we wish to consider. They were also calculated to be the most stable defects comprising fewer than five lattice species.

3. Computational technique

(*a*) *Mott–Littleton methodology*

This procedure is based upon a description of the lattice in terms of effective potentials. The crystal lattice is partitioned into two regions: an inner region I that includes a defect at its centre and an outer region II which extends to infinity (see figure 4). In region I, interactions are calculated explicitly and all ions are relaxed to zero force. We consider interactions due to long-range Coulombic effects (assuming formal charges on all ions) and also short-range forces that are modelled using parametrized pair potentials (see Appendix A). The response of region II is treated using the Mott–Littleton approximation (Mott & Littleton 1938). In this work, the CASCADE code was used for all calculations (Leslie 1982).

The relaxed positions of ions in region I are determined using a Newton–Raphson minimization technique as outlined by Norgett & Fletcher (1970). To ensure a smooth transition between regions I and II, we incorporate an interfacial region IIa in which ion displacements are determined via the Mott–Littleton approximation but in which interactions with ions in region I are calculated by explicit summation. In the present calculations region I has a radius of 4.2 lattice units (445 ions) and region IIa extends out to 7.2 lattice units and incorporates an additional 1800 ions. Region sizes were chosen to be large enough to ensure that no appreciable change in

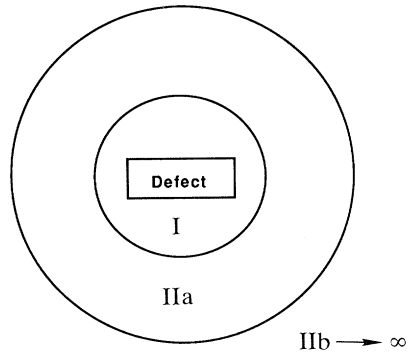

Figure 4. The two-region methodology used in Mott–Littleton calculations.

defect formation energy occurs if the region sizes are increased further. The effect of region size on defect energy has been discussed in previous studies (Catlow 1977; Jackson *et al.* 1986; Grimes & Catlow 1990).

Long-range coulombic interactions are summed using Ewald's method for a defective lattice (Norgett 1974). Short-range potentials were calculated using the electron-gas methodology (Harding & Harker 1982; see also Appendix A) and with a suitable choice of parameters (A, ρ, and C), fitted to the Buckingham potential form:

$$V(r) = A \exp(-r/\rho) - C/r^6.$$

These potentials model the effect of electron cloud overlap and dispersion interactions, both of which are negligible beyond a few lattice spacings. The Buckingham potential is therefore a suitable choice since both exponential and r^{-6} terms decay quickly with increasing distance. As such, we need only consider a finite number of the short-range interactions for each ion in the unit cell. This is achieved by defining a short-range cut-off parameter (in this case 4.2 lattice units) beyond which short-range interactions are set to be zero.

(*b*) *The shell model*

Ionic polarization effects are described using the shell model of Dick & Overhauser (1958), which has been widely used in both lattice dynamical (Cochran 1973) and defect calculations (Catlow 1977; Catlow & Mackrodt 1982). The model describes an ion in terms of a massless shell of charge Y surrounding a massive core of charge X. The formal charge state of an ion is therefore equal to $(X+Y)$. The core and shell charges are coupled by means of an isotropic harmonic spring of force constant k. Polarization of an ion can then occur through the displacement of the shell relative to the core. The choice of shell model parameters is discussed in Appendix A. Justification for this approach comes from the success of the model in predicting experimental lattice properties (table 8), in particular, phonon dispersion curves (Harding *et al.* 1980; Jackson *et al.* 1986).

Recently, a systematic comparison of classical Mott–Littleton and quantum mechanical Hartree–Fock methods has been carried out by calculating the formation energy of point defects in MgO (Grimes *et al.* 1989*a*) and the solution energies of inert gas atoms in UO_2 (Grimes *et al.* 1989*b*). An acceptable level of agreement was found between these different methods thereby lending support to the classical approach.

Ultimately, justification for this simulation technique comes from its success in investigating a diverse range of problems in oxide materials. Of relevance to the

present study is the modelling of extensive non-stoichiometry in $Fe_{1-x}O$ (Catlow & Fender 1975; Tomlinson *et al.* 1990) and TiO_{2-x} (Catlow & James 1982). Also, there have been successful predictions of the structure and stability of zeolites (Jackson & Catlow 1988) and other alumino-silicates such as clays and micas (Collins & Catlow 1990) all of which are expected to show significant covalency.

4. Previous theoretical studies

Previous computer modelling studies of UO_2 have concentrated on the derivation of adequate interatomic potentials and on the description of defect structures and non-stoichiometry (Catlow 1977*a*; Catlow 1978; Jackson *et al.* 1986). These studies have clearly established the viability of computer modelling techniques for calculating defect formation, clustering and migration energies in UO_2. Initial studies of fission product behaviour were confined to investigations of Xe in UO_2. Detailed studies by Jackson & Catlow (1985*a*, *b*), following the earlier work of Catlow (1978), determined the sites occupied by the inert gas atoms, established the dependence of site occupancy on stoichiometry and showed that the solution energy of Xe in UO_2 is large and unfavourable.

In more recent work, Grimes *et al.* (1989*c*) reconsidered the solubility of Xe and calculated solution energies for Ne, Ar, Kr, Cs, Ba, Rb, Sr, Br and I. In addition the possibility of charge transfer from fission products to the lattice was investigated. The present study extends this earlier work in four important respects: firstly, we consider solution at more complex sites; secondly, we examine the equilibrium that exists between solution sites; third we include the effect of stoichiometry on solution processes. Fourth, we consider solution not simply with respect to gas phase ions but also the possibility of an alternative oxide or molecular state for a fission product. Inclusion of these effects allows us to explore comprehensively the chemical state of the more important fission products.

5. Results and discussion

(*a*) *Solution energies for* Cs, Rb, Ba, Sr, La, Y, Ce, Zr, Xe *and* Kr

In this section we use calculated energies to examine the solution of fission products. Initially we shall consider the incorporation energy of a fission product at a pre-existing trap site. The formation of the trap (or solution) site is then included in the calculations. The last part of the model involves the equilibrium between fission products dissolved in the fuel and those precipitated as binary oxides.

(i) *Definition of incorporation energy*

We wish to determine the stability of fission products trapped (or bound) at pre-existing trap sites. This is achieved by calculating incorporation energies which are defined in this context to be the energy to trap a fission product atom or ion initially assumed to be at infinity, to a pre-existing solution site.

In practice the Mott–Littleton methodology requires that we calculate both the substitution energy of the fission product at the solution site and the energy to form the solution site so that

$$\left\{\begin{matrix}\text{incorporation}\\ \text{energy}\end{matrix}\right\} = \left\{\begin{matrix}\text{fission product}\\ \text{substitution energy}\end{matrix}\right\} - \left\{\begin{matrix}\text{solution site}\\ \text{formation energy}\end{matrix}\right\}.$$

Thus a positive result means that energy is required to incorporate the ion in the solid whereas a negative energy implies that incorporation is energetically favourable. It is important to emphasize that in this definition, the thermodynamic zero of the fission product is a gas-phase atom or ion in the same electronic state as in the solid.

Comparison of incorporation energies is the simplest way by which fission product stability may be assessed. However, use of the incorporation energy function is limited since it is not sensitive to any equilibrium between trap sites and hence does not change with fuel stoichiometry. In addition, a free ion thermodynamic zero is not usually physically realistic. Nevertheless, the incorporation energy can be used to predict the most stable trap site for a fission product provided that all trap sites are available for occupation and the fission product is already present in the fuel. This will be the situation when the concentration of fission products is low enough that incorporation proceeds through occupation of pre-existing defect sites; that is, it is not necessary for the fission product to create its own defect site. However, since such small concentrations of fission products only occur in fuels of extremely low burn-up, we shall not discuss these results further; they have been considered in previous publications (Grimes 1988; Grimes *et al.* 1989*c*).

(ii) *Definition of solution energy*

In any reasonable concentrations, fission products must be accommodated at extrinsic trap sites and the equilibrium between trap sites must be included in solution energy calculations: that is, since trap sites must be created to accommodate the fission products, the formation energy of the trap is necessarily a component of the solution energy. The equation governing extrinsic solution is, therefore,

$$\left\{\begin{array}{c}\text{solution energy}\\ \text{(in equilibrium with}\\ \text{solution sites)}\end{array}\right\} = \left\{\begin{array}{c}\text{incorporation}\\ \text{energy}\end{array}\right\} + \left\{\begin{array}{c}\text{formation energy of}\\ \text{the equilibrium}\\ \text{solution site}\end{array}\right\}.$$

Formation energies of equilibrium solution sites are a function of fuel stoichiometry and hence of burn-up. The energy dependence has been investigated by considering changes in the equilibrium between Schottky and oxygen Frenkel disorder. Solution site formation energies calculated for UO_{2-x}, UO_2 and UO_{2+x} are presented in table 10. The details of these calculations are discussed in Appendix B. Implicit within this model is the assumption that the system is at thermodynamic equilibrium and that the fission products do not interact with each other.

We should stress that solution energies are defined with respect to atoms or ions at rest and at infinity. Negative values would therefore be expected for the incorporation of ions into the polar UO_2 lattice.

(iii) *Inert gas atoms*

The solution energies are presented in table 2; for each stoichiometry, the lowest solution energy is italicized. In UO_{2-x} the calculations suggest that the tri-vacancy trap provides the lowest solution energies for Xe and Kr. This is a consequence of the relative ease with which the large gas atoms can be incorporated into the large tri-vacancy site and the relatively low formation energy of the tri-vacancy in UO_{2-x} compared with other suitable trap sites (see table 10).

In UO_2, the reduction of the di-vacancy trap formation energy makes it much

Table 2. *Solution energies of fission products (electronvolts)*

stoichiometry:	UO_{2-x}	UO_2	UO_{2+x}	UO_{2-x}	UO_2	UO_{2+x}	UO_{2-x}	UO_2	UO_{2+x}	UO_{2-x}	UO_2	UO_{2+x}
	(*a*) Xenon			(*b*) Caesium			(*c*) Barium			(*d*) Lanthanum		
oxygen vacancy	13.34	16.75	20.16	9.10	12.51	15.92	−4.44	−1.03	2.38	−27.55	−24.14	−20.72
uranium vacancy	18.32	11.50	*4.68*	7.26	*0.43*	*−6.39*	−10.04	*−16.87*	*−23.69*	−39.00	*−45.82*	*−52.65*
di-vacancy	12.93	*9.52*	6.11	4.47	1.06	−2.35	*−11.63*	−15.04	−18.45	*−39.73*	−43.14	−46.56
neutral tri-vacancy	*9.57*	*9.57*	9.57	*2.94*	2.94	2.94	*−11.61*	−11.61	−11.61	−38.63	−38.63	−38.63
charged tetra-vacancy	19.78	12.96	6.13	11.22	4.40	−2.42	−2.48	−9.30	−16.13	−31.70	−38.52	−45.34
interstitial	17.23	17.23	17.23	9.93	9.93	9.93	−3.33	−3.33	−3.33	−31.14	−31.14	−31.14
	(*e*) Cerium			(*f*) Krypton			(*g*) Rubidium					
oxygen vacancy	−59.02	−55.61	−52.20	9.93	13.34	16.75	5.97	9.38	12.79			
uranium vacancy	*−73.16*	*−79.98*	*−86.80*	17.23	10.31	*3.48*	5.93	*−0.89*	*−7.72*			
di-vacancy	*−73.34*	−76.75	−80.17	12.49	*9.08*	5.67	3.39	−0.02	−3.43			
neutral tri-vacancy	−71.41	−71.41	−71.41	*9.49*	9.49	9.49	*2.29*	2.29	2.29			
charged tetra-vacancy	−65.11	−71.93	−78.75	19.11	12.29	5.47	10.54	3.71	−3.11			
interstitial	−63.25	−63.25	−63.25	13.31	13.31	13.31	6.38	6.38	6.38			
	(*h*) Strontium			(*i*) Yttrium			(*j*) Zirconium					
oxygen vacancy	−8.87	−5.46	−2.05	−32.67	−29.26	−25.85	−70.37	−66.96	−63.54			
uranium vacancy	−13.76	*−20.58*	*−27.41*	−41.49	*−48.31*	*−55.14*	−79.67	*−86.50*	*−93.32*			
di-vacancy	*−15.22*	−18.63	−22.04	*−42.30*	−45.71	−49.12	*−80.49*	−83.90	−87.31			
neutral tri-vacancy	−14.95	−14.95	−14.95	−41.26	−41.26	−41.26	−79.21	−79.21	−79.21			
charged tetra-vacancy	−7.34	−14.17	−20.99	−34.24	−41.07	−47.89	−72.72	−79.54	−86.36			
interstitial	−11.04	−11.04	−11.04	−36.40	−36.40	−36.40	−74.25	−74.25	−74.25			

easier to form than the tri-vacancy. As a result, we predict that solution of Xe in UO_2 can occur at both di- and tri-vacancy sites. In this context we note that solution at either the di- or tri-vacancy sites will result in Xe being displaced from a regular cation site. This is in agreement with the experimental data of Matzke (1980).

Kr in UO_2 behaves differently from Xe in so far as solution at the di-vacancy site is favoured over that for the tri-vacancy site. However, the Kr atom will still be displaced from the lattice site.

Further oxidation of the fuel to UO_{2+x} is accompanied by a significant decrease in the uranium vacancy formation energy (see table 10). This leads to a greater preference for Xe and Kr to occupy single vacancy sites (see table 2).

(iv) *Metal cations*

The results for gas atoms can be understood in terms of a balance between atom size, solution site size and the energy required to form the solution site. To understand cation solution we must also consider the influence of the variable cation charge and its interaction with the different apparent charges of the solution sites (see figure 3). The coulombic effects will of course be greatest for the higher charged cations interacting with the higher charged sites (e.g. Zr^{4+} at the uranium vacancy site). Usually, ion size and charge effects tend to reinforce each other since the highest charged cations are also the smallest. Hence the higher charged cations are more readily accommodated at the smaller trap sites. Thus, if we consider the solution of Cs^+ and Ce^{4+} in UO_{2-x} (see table 2), the calculations predict that Cs^+ will occupy a neutral tri-vacancy trap whereas the solution energy for Ce^{4+} is lowest at a (4− charged) uranium vacancy.

In UO_2 and UO_{2+x}, solution energies are lowest when trapping occurs at the uranium vacancy site. In UO_{2+x} this is encouraged by the fact that the uranium vacancy has the lowest effective formation energy (see table 10). In UO_2, although the doubly charged di-vacancy and uranium vacancy have similar effective formation energies, the greater Madelung potential and the higher charged uranium vacancy site overcomes the ion size considerations which would favour solution at the larger di-vacancy trap.

In summary, the calculations predict that only in UO_{2-x} does competition between charge, size and trap formation lead to solution at di- or tri-vacancy sites. Solution of the cations at oxygen vacancies, charged tetra-vacancies or at the interstitial site is never favoured.

As for the case of the inert gases, there is little direct experimental data with which to test our cation solution site predictions. However, a channelling study (Matzke & Blank 1989) suggests that in UO_2, Rb and Cs occupy lattice sites: our calculations are consistent with these conclusions (see table 2).

(v) *Solution from fission product binary oxides*

Calculated solution energies are useful in predicting the extrinsic solution site occupancy of fission products in nuclear fuels. However, these results cannot be used to determine whether the fission product will precipitate out of solution in a more stable second phase. Although there are a great number of possible second phase materials that the fission products might form both with each other and with components of the UO_2 host, experimental data suggest that the majority of these are oxides. We have therefore chosen to calculate the solubility of fission product binary oxides in UO_2. However, this is not intended to provide a complete model for

PHILOSOPHICAL TRANSACTIONS OF THE ROYAL SOCIETY A MATHEMATICAL, PHYSICAL & ENGINEERING SCIENCES

fission product precipitation since more complex phases (some of which will be investigated in the next section) are also important in the solution equilibria. Nevertheless, we believe that these results contain the salient features that control grey phase precipitation.

We can calculate the energies required to dissolve possible binary oxide precipitates in UO_2, by considering the following relationship:

$$\left\{\begin{matrix}\text{solution energy}\\ \text{of precipitate}\end{matrix}\right\} = \left\{\begin{matrix}\text{latice energy of}\\ \text{oxide precipitate}\end{matrix}\right\} + \left\{\begin{matrix}\text{fission product}\\ \text{solution energy}\end{matrix}\right\} + \left\{\begin{matrix}\text{solution energy}\\ \text{of oxide ion into}\\ \text{UO}_2\text{ host}\end{matrix}\right\}.$$

The relevant lattice energies have been calculated and are reported in table 9. The solution energies of fission product ions have been previously calculated. We also require that in addition to solution of the fission product, the additional oxygen ions which arise from the decomposition of the precipitate are also incorporated. In UO_{2-x}, this results in the solution of oxygen ions at oxygen vacancy sites. For UO_{2+x}, we expect oxygen to substitute interstitially and in UO_2, oxygen is equally divided between interstitial and vacancy sites.

The solution process can be understood more clearly if we consider in detail the process of solution of Cs_2O in UO_2. The first component in the solution process is the *decomposition of fission product oxide*:

$$Cs_2O \longrightarrow 2Cs^+(g) + O^{2-}(g).$$

This is independent of the fuel stoichiometry.

The second step is to form the trap sites necessary to incorporate the Cs^+ and O^{2-} ions. In UO_{2-x}, the most favourable equilibrium trap site is the neutral tri-vacancy (NTV); in UO_2 and UO_{2+x}, solution occurs at a uranium vacancy (V_U''''). Since it is necessary to form two cation solution sites to accommodate one formula unit of Cs_2O, trap formation follows from the following.

Formation of trap site:

UO_{2-x}: $$2Cs^+(g) + O^{2-}(g) + 2\text{NTV} + V_O^{\cdot\cdot} \longrightarrow 2Cs_{\text{NTV}}^{\cdot} + O_O^{\times},$$

UO_2: $$2Cs^+(g) + O^{2-}(g) + 2V_U'''' + \tfrac{1}{2}V_O^{\cdot\cdot} \longrightarrow 2Cs_U''' + \tfrac{1}{2}O_O^{\times} + \tfrac{1}{2}O_i'''',$$

UO_{2+x}: $$2Cs^+(g) + O^{2-}(g) + 2V_U'''' \longrightarrow 2Cs_U''' + O_i''.$$

The energies required for trap formation are presented in table 10.

Lastly, we incorporate the Cs^+ and O^{2-} into the trap sites.

Incorporation of fission product and associated oxygen into vacant trap sites:

UO_{2-x}: $$2Cs^+(g) + O^{2-}(g) + 2\text{NTV} + V_O^{\cdot\cdot} \longrightarrow 2Cs_{\text{NTV}}^{\cdot} + O_O^{\times},$$

UO_2: $$2Cs^+(g) + O^{2-}(g) + 2V_U'''' + \tfrac{1}{2}V_O^{\cdot\cdot} \longrightarrow 2Cs_U''' + \tfrac{1}{2}O_O^{\times} + \tfrac{1}{2}O_i'',$$

UO_{2+x}: $$2Cs^+(g) + O^{2-}(g) + 2V_U'''' \longrightarrow 2Cs_U''' + O_i''.$$

The results of binary oxide solution are presented in table 3: a positive energy indicates that the oxide is insoluble in the fuel. It is also important to bear in mind that these energies are sensitive to the energies of trap formation for cations and anions, the Coulomb attraction between cations and trap sites and ion size effects. We shall use these concepts to explain some of the trends in solution energies observed in table 3.

Table 3. *Solubility of secondary phases in fuel (electronvolts per formula unit)*

	fuel stoichiometry		
oxide	UO_{2-x}	UO_2	UO_{2+x}
Cs_2O	10.58	8.98	−1.25
Rb_2O	10.11	7.18	−3.05
BaO	3.57	1.74	−1.68
SrO	2.43	0.48	−2.93
La_2O_3	1.52	−0.43	−3.84
Y_2O_3	1.31	−0.48	−3.89
ZrO_2	0.21	1.03	1.03
CeO_2	−0.11	0.07	0.07
CsI	17.79	16.49	2.13
CsBr	18.32	17.76	2.62
Cs_2Te	25.75	23.05	−2.02
Xe	9.57	9.52	4.68
Kr	9.49	9.08	3.48

A consideration of the relative ion sizes is enough to explain the differences between the solution energies of the oxides Cs_2O and Rb_2O; BaO and SrO; La_2O_3 and Y_2O_3; or ZrO_2 and CeO_2. For each pair, the Coulomb interactions between the cations and the solution site is identical. Thus, for each pair, the oxide whose cation is closest in size to the U^{4+} ion is the most soluble.

Now let us examine the trends in solution energy between oxides that have different cation charges. In UO_{2-x}, the results suggest that the solution energies of the oxides are ordered so that $A_2O < BO < C_2O_3 < DO_2$. The order remains the same when we consider the solution energies per cation. Thus, at first sight, it seems as if the solution energies are a simple function of cation charge. However, this is misleading because the equilibrium trap site in UO_{2-x} is the neutral tri-vacancy and consequently there is no long-range Coulombic attraction of charged cations. The charge of the cation *per se* is therefore not the important factor in deciding the relative solubility of the oxide. We recall that the stability of the tri-vacancy in UO_{2-x} is due to the fact that oxygen vacancies are the dominant defects in UO_{2-x}. The large population of oxygen vacancies also makes the incorporation of oxygen from the fission product oxide into UO_{2-x} energetically favourable since these anions will occupy the vacancy sites. Now, an oxide such as $\frac{1}{2}(A_2O)$ can only provide $\frac{1}{2}O^{2-}$ ions per A cation, whereas BO provides one O^{2-}, $\frac{1}{2}(C_2O_3)$ provides $\frac{3}{2}O^{2-}$ ions and DO_2 provides $2O^{2-}$ ions. Therefore, the relative solution energy of the oxide follows from the number of O^{2-} ions that the oxide can provide to the lattice. The same argument also explains why the solution energies for Xe and Kr are even higher since they provide no O^{2-} ions.

In UO_{2+x}, the equilibrium trap site for all cations is the uranium vacancy. Since this has a charge of 4−, the trap has a strong preference for higher charged cations. The component of the solution energy arising from cation solution will therefore be greater for oxides with higher oxygen:metal ratios. However, the difficulty in incorporating the additional O^{2-} ions from the fission product oxide into UO_{2+x} makes the solution energies of oxides with higher oxygen:metal ratios less favourable. The reason for O^{2-} ions having high incorporation energies in UO_{2+x} is that these ions must occupy interstitial sites and this is energetically less

favourable. Thus, the components of the solution energy that are derived from cation charge compensation of the V_U'''' trap and those from the solution of the additional O^{2-} ions largely balance out and only small variations in the solution energies remain.

These general considerations can be used to explain the variation in solution of the different oxides. In addition, we can test the predictions by comparison with the experimental data reviewed in the Introduction. For example, we noted that a greater amount of Cs is retained in fuels with higher oxygen : metal ratios (Phillips *et al.* 1974). Our prediction of the increasing solubility of Cs_2O as one goes from hypo- to hyper-stoichiometric UO_2 is in agreement with this observation.

The model also successfully predicts that Y_2O_3, La_2O_3 and CeO_2 are all soluble in UO_2. However, the calculations suggest that Y_2O_3 and La_2O_3 will not be soluble in UO_{2-x}; no data are presently available to test this. We note that the greater solubility of CeO_2 over ZrO_2 in UO_2 is also supported by the available experimental data.

Experimental data for the solubility of Sr are known for both UO_{2-x} and UO_2. They show that Sr is an order of magnitude more soluble in UO_2 than in UO_{2-x} (Kleykamp 1985). Again the calculations mirror this trend. The experimental observation, discussed in the Introduction, that Ba is less soluble than Sr also lends support to our calculated values.

The value of the model is now apparent. It highlights trends in site preference and solution energy, makes predictions where experimental data are not available and it provides a theoretical framework within which the behaviour of the fission products may be understood.

(vi) *Reactions between fission product oxides*

In the present study it is not possible to consider all the possible reactions that might occur between the component fission product binary oxides. Nevertheless it is useful to investigate some such reactions and to show that useful results can be obtained. Therefore, we have restricted our investigation to one particular subset of reactions: those that occur between BaO and either UO_2 or ZrO_2 and those between SrO and either UO_2 or ZrO_2. All the reactions are assumed to form perovskite phases of the general formula ABO_3. These reactions were chosen because the final products are related to grey phase precipitates observed experimentally, as discussed in the Introduction.

The results for these reactions are given in table 4. Since a positive reaction energy is calculated for the reaction between SrO and UO_2, we do not predict the formation of $SrUO_3$. However, $BaZrO_3$, $SrZrO_3$ and $BaUO_3$ are stable with respect to the corresponding binary oxides. The model reproduces the experimental lattice parameters for the three stable perovskite oxides to within 1%. The failure to date to prepare $SrUO_3$ supports our prediction of its instability.

The second point to note is that the energies calculated for these reactions would not perturb the binary oxide solution energies enough to change the general conclusions concerning solubility. For example, we still predict that Sr will be soluble in UO_{2+x} despite the possibility of its incorporation into the more stable $SrZrO_3$ phase. (The solubility of $SrZrO_3$ can easily be calculated by summing the solution energies of the component binary oxides and subtracting the energy for the oxide–oxide reaction.) Since these perovskite-type phases are the most commonly observed oxide precipitates in high burn-up fuels (Kleykamp *et al.* 1985) it is

Table 4. *Formation of complex oxides from fission products*
(A negative sign indicates that the reaction is exothermic.)

$BaO + UO_2 \longrightarrow BaUO_3$	$\Delta E = -0.18$ eV
$BaO + ZrO_2 \longrightarrow BaZrO_3$	$\Delta E = -0.48$ eV
$SrO + UO_2 \longrightarrow SrUO_3$	$\Delta E = +0.60$ eV
$SrO + ZrO_2 \longrightarrow SrZrO_3$	$\Delta E = -0.60$ eV

reasonable to assume that their formation energies will be close to those of the most favourable form for any grey phase precipitate. This being so, the results suggest that the trends in solubility for the cations are characterized by the solubility of the corresponding binary oxides. Thus, given the fuel stoichiometry, the results reported in table 3 can be used to predict whether it is likely that a fission product cation will be dissolved in the fuel or precipitated out of solution as a component of a secondary phase, mixed metal oxide. The stability of oxide precipitates will be the focus of more extensive investigation in future work.

(*b*) *Solution energies for fission products with variable charge states*: I, Br, Te *and* Xe

If fission products can exhibit variable charge states, there will be important implications for the redox properties of the fuel. In particular, as the oxygen potential increases, fission products may buffer the oxidation reaction and help to keep the charge of the uranium ions closer to four. In extreme circumstances, oxidation of fission products might prevent structural phase changes to higher oxides such as U_4O_9 and thereby help to maintain the structural integrity of the fuel.

To investigate the possibility of fission product oxidation, we must consider the relative stability of different charge states. This is achieved by including, in the solution energy calculations, the ionization energy required to create the new charge. Thus if an ion A is oxidized from charge state n to charge state m, we define the relative solution energy with respect to the starting species by:

$$\left\{\begin{matrix}\text{relative solution}\\ \text{energy}\end{matrix}\right\} = \left\{\begin{matrix}\text{solution}\\ \text{energy}\end{matrix}\right\} - \sum_{i=n}^{m} \left\{\begin{matrix}i\text{th ionization}\\ \text{energy}\end{matrix}\right\} + (n-m)\left\{\begin{matrix}\text{electron}\\ \text{affinity}\end{matrix}\right\}$$

(the ionization energies are taken from Moore (1971) as tabulated in the CRC Handbook (1987)). The starting point for ionization of the fission product has been defined with respect to the charge state of the fission product in the appropriate phase outside the fuel; that is, Xe° (gas phase), I^- (CsI), Br^- (CsBr), and Te^{2-} (Cs_2Te).

Ionization is defined in terms of electrons being removed to infinity. In a real material, the electrons are not removed from the fuel. We must therefore include an energy, the electron affinity of the lattice, which corresponds to the gain in energy that occurs as a result of the incorporation of an additional electron into the lattice. The value of the electron affinity will be a function of the fuel stoichiometry. In this study, we consider values for the electron affinity in UO_{2-x}, UO_2 and UO_{2+x}.

The upper value corresponds to an oxygen-*excess* fuel, UO_{2+x}, in which there are electron holes in the valence band. The lower value corresponds to an oxygen-*deficient* fuel, UO_{2-x}, which has electrons in the condution band. The difference between the electron affinity of these fuels will be the thermal band gap energy. The experimental value for this is 2.3 eV (Bates *et al.* 1967). If we asume that the

conduction band in UO_{2-x} is close to the vacuum, we can approximate the affinity of UO_{2-x} as zero. Consequently, the electron affinity of UO_{2+x} is 2.3 eV and that of UO_2 is 1.15 eV, since half the electrons will be captured by hole states and the remainder will be in the conduction band.

(i) *The charge state of* Xe

The oxidation of Xe° to Xe^+ was investigated for stoichiometries corresponding to UO_{2-x}, UO_2 and UO_{2+x}. In each case, the solution energies for Xe° and Xe^+ were calculated at each of the six solution sites. The results are presented in table 5*a*. For each solution site, the lowest energy indicates the most favourable charge state for that solution site. The lowest solution energy for each stoichiometry (the site we predict to be occupied) is italicized. It is possible to draw conclusions as to the fission gas charge state from the results in table 5*a* because the solution energies include the energy components necessary to oxidize Xe from Xe° to Xe^+ and to incorporate the resulting electron into the lattice. The results in table 5 can therefore be used as a 'reference' table with the differences in solution energies (at constant stoichiometry) corresponding to the energies gained or lost when Xe is transferred between different sites and/or charge states.

In UO_{2-x}, we predict that Xe remains as a neutral atom in the tri-vacancy; in UO_2 Xe will also maintain its neutral charge state and will occupy either a neutral tri-vacancy or the di-vacancy traps. However, in UO_{2+x}, the possibility of oxidation to Xe^+ is realized. This is because the most favourable solution site is the uranium vacancy and this has a great affinity for positively charged ions. Consequently, the Madelung potential at this site combined with the 2.3 eV electron affinity of the lattice are great enough to overcome the first ionization energy of Xe and form Xe^+. However, the excess solution energy of Xe^+ over Xe° at the uranium vacancy site is only 1.3 eV. Thus, it would be possible for perturbations such as other defects in the vicinity of the trap, to reduce the Madelung potential of the trap site sufficiently to prevent the oxidation of Xe°. The conclusion is therefore that only in UO_{2+x} is Xe likely to be oxidized to Xe^+ and that ionization in UO_2 can be ruled out.

(ii) *The charge state of* I *and* Br

The values in table 5*b* and *c* can be used to predict the most stable charge states of I and Br under different oxidation conditions. The reference charge states of I and Br were chosen to be I^- and Br^- since we shall investigate the solution of CsI and CsBr in a later section.

In UO_{2-x}, I and Br are most stable as anions trapped at oxygen vacancy sites. This is encouraged by the ease of forming the oxygen vacancy trap and the low electron affinity of UO_{2-x} (see table 10). In UO_2, the negative and neutral charge states of I and Br have similar solution energies. The equilibrium trap sites in UO_2 are the di-vacancies and neutral tri-vacancies. The most favourable trap site for I and Br in UO_{2+x} is the uranium vacancy. Consequently, I and Br assume positive charge states. It is important to note that in UO_{2+x}, the positive charge states of these ions exhibit solution energies that are over 2 eV lower than the neutral atoms and over 4 eV lower than would be the case if they were forced to assume a negative charge state. Thus we can make the firm prediction that the charge states of I and Br are functions of the fuel stoichiometry.

In future work we aim to study the formation of higher charge states. Preliminary results suggest that I^{2+} will be more stable than I^+ in UO_{2+x} but that Br^{2+} will be less

PHILOSOPHICAL TRANSACTIONS OF THE ROYAL SOCIETY A MATHEMATICAL, PHYSICAL & ENGINEERING SCIENCES

Table 5. *Solution energies for* Xe, I, Br *and* Te (*electronvolts*)

stoichiometry:	UO_{2-x}		UO_2		UO_{2+x}	
charge state:	0	1+	0	1+	0	1+
(*a*) **Xenon**						
oxygen vacancy	13.34	20.65	16.75	22.91	20.17	29.77
uranium vacancy	18.32	19.33	11.50	11.35	4.68	*3.38*
di-vacancy	12.93	16.54	*9.52*	11.98	6.11	7.42
neutral tri-vacancy	*9.57*	14.99	*9.57*	13.84	9.57	12.69
charged tetra-vac.	19.78	23.26	12.96	15.29	6.13	7.31
interstitial	17.23	21.92	17.23	20.77	17.23	19.62

stoichiometry:	UO_{2-x}			UO_2			UO_{2+x}		
charge state:	1−	0	1+	1−	0	1+	1−	0	1+
(*b*) **Iodine**									
oxygen vacancy	*8.92*	13.87	22.30	12.34	16.13	23.42	15.75	18.39	24.53
uranium vacancy	22.14	20.86	20.84	15.32	12.89	11.72	8.49	4.91	*2.59*
di-vacancy	14.54	14.67	18.05	11.13	*10.13*	12.34	7.07	5.57	6.62
neutral tri-vacancy	10.44	13.44	16.50	10.39	12.29	14.20	10.39	11.14	11.90
charged tetra-vac.	21.40	22.56	24.77	14.58	14.58	15.64	7.75	6.61	6.52
interstitial	15.77	17.24	23.39	15.77	16.09	21.09	15.77	14.94	18.79
(*c*) **Bromine**									
oxygen vacancy	*8.83*	12.38	20.64	12.24	14.64	21.75	15.65	16.90	22.86
uranium vacancy	22.08	20.49	20.71	15.26	12.52	11.59	8.44	4.55	*2.46*
di-vacancy	14.19	15.67	18.19	*10.78*	*11.10*	12.48	7.37	6.54	6.77
neutral tri-vacancy	11.09	13.41	17.14	*11.09*	12.26	14.84	11.09	11.11	12.54
charged tetra-vac.	21.81	22.50	25.43	14.99	14.52	16.31	8.17	6.55	7.18
interstitial	14.42	15.45	20.80	14.42	14.30	18.50	14.42	13.15	16.20

stoichiometry:	UO_{2-x}					UO_2				
charge state:	2−	1−	0	1+	2+	2−	1−	0	1+	2+
(*d*) **Tellurium**										
oxygen vacancy	*1.77*	8.37	11.41	18.24	22.16	5.18	10.64	12.52	18.20	20.97
uranium vacancy	21.29	21.23	17.94	16.66	15.51	14.46	13.25	8.82	6.39	*4.09*
di-vacancy	14.85	15.40	12.05	13.89	13.93	11.44	10.84	6.34	7.03	5.92
neutral tri-vacancy	12.82	9.62	10.80	12.38	13.97	12.82	8.47	8.50	8.90	9.37
charged tetra-vac.	18.99	20.53	20.00	20.68	21.58	12.17	12.55	10.87	10.41	10.16
interstitial	10.81	15.08	14.14	19.04	20.35	10.81	13.93	11.84	15.59	15.65

stoichiometry:	UO_{2+x}				
charge state:	2−	1−	0	1+	2+
oxygen vacancy	5.18	12.90	13.64	18.17	19.78
uranium vacancy	7.64	5.28	−0.31	−3.88	*−7.34*
di-vacancy	8.02	6.27	0.63	1.31	−2.09
neutraltri-vacancy	12.82	7.32	6.20	5.48	4.77
charged tetra-vac.	5.34	4.58	1.75	0.13	−1.27
interstitial	10.81	12.78	9.54	12.14	11.05

PHILOSOPHICAL TRANSACTIONS OF THE ROYAL SOCIETY A MATHEMATICAL, PHYSICAL & ENGINEERING SCIENCES

stable than Br^+. This is a consequence of the higher ionization energies exhibited by Br.

(iii) *The charge state of* Te

In table 5*c* we present the solution energies for five charge states of Te. The lowest solution energy calculated in UO_{2-x} is for Te^{2-} at an oxygen vacancy trap. The 2− charge has been chosen as the reference state for Te since we will investigate the solution of Te from Cs_2Te. In UO_2 and UO_{2+x}, the most stable solution site is the uranium vacancy and in this trap, Te exhibits a charge state of 2+. The result for UO_2 is supported by recent channelling experiments which showed that Te occupies a lattice site. Indeed we suggest that Te occupies a lattice site at all stoichiometries although the site varies with stoichiometry.

As with Br and I, we conclude that the charge state of Te will depend on the fuel stoichiometry. In fact, the variation with Te is greater than for I and Br as solution of Te^{2-} in UO_{2-x} and solution of Te^{2+} in UO_{2+x} are particularly favoured.

(iv) *Solution of* CsI, CsBr *and* Cs_2Te

In table 3 we present the solution energies of the Cs compounds of I, Br and Te. For each material, the calculations include the variation that solution sites and charge states exhibit as a function of stoichiometry. Although the details of the behaviour are complex, the resulting energies, presented in tables 2 and 5, can be used in a simple manner to determine the solution energies of possible compounds. For example, consider the solution of CsI. In table 2*b*, at each stoichiometry, we find the lowest solution energies for Cs. These are added to the lowest solution energies for I reported in table 5*b*, at the corresponding stoichiometry. The charge state of I chosen from the results in table 5*b* does not have to be −1 as all energies are calculated assuming the initial solution of I^- with the subsequent full electronic rearrangement of charge (in equilibrium with the lattice) to the appropriate charge state. The sum of the two solution energies corresponds to solution from the gas phase ions Cs^+ and I^-. The energy to form the gas phase ions from CsI is simply the lattice energy reported in table 9. Thus, in general, at a given stoichiometry,

$$\left\{\begin{matrix}\text{solution energy}\\ \text{of compound}\\ \mathrm{A}_n\,\mathrm{B}_m\end{matrix}\right\} = \left\{\begin{matrix}n\times\text{solution}\\ \text{energy of ion A}\end{matrix}\right\} + \left\{\begin{matrix}m\times\text{solution}\\ \text{energy of ion B}\end{matrix}\right\} - \left\{\begin{matrix}\text{lattice energy}\\ \text{of } \mathrm{A}_n\,\mathrm{B}_m\end{matrix}\right\}.$$

The results in tables 2, 5 and 9 can provide an efficient way of calculating the solution energies of many different compounds of fission products so long as it is possible to calculate the lattice energy of the binary compound.

The results for the solution of CsI and CsBr are presented in table 3. We predict that solution of these compounds in the fuel is never favoured. Conversely, solution of Cs_2Te in UO_{2+x} will occur although not in UO_2 and UO_{2-x}. Thus, at full thermodynamic equilibrium, I and Br will completely precipitate out from the fuel in combination with Cs. However, since the amount of Cs produced during fission is significantly greater than the combined amount of I and Br (see figure 1), we still expect some Cs to remain in UO_{2+x} (or to precipitate out in other secondary phases yet to be investigated).

PHILOSOPHICAL TRANSACTIONS OF THE ROYAL SOCIETY A MATHEMATICAL, PHYSICAL & ENGINEERING SCIENCES

6. Summary and conclusions

The aim of this work has been to develop a theoretical model that incorporates all the features necessary to simulate the solution properties of fission products in uranium dioxide fuel at thermodynamic equilibrium. In so doing, we hope to have provided some of the explanations of the significant range of behaviour exhibited by different fission products.

The calculations were at an atomistic level. The first part of the model considered solution of fission product species at pre-existing trap sites. Since the concentration of fission products will be greater than the population of intrinsic trap sites, we next included the energy to form trap sites. This was accomplished by calculating the trap site equilibria with respect to the Schottky and Frenkel defects. This is a function of the fuel stoichiometry. The resulting solution energies were used to predict the most stable solution sites for Xe, Kr, Cs, Rb, Ba, Sr, La, Y, Ce and Zr in UO_{2-x}, UO_2 and UO_{2+x}.

Generally it was found that the most stable solution site depended on the fuel stoichiometry. In UO_{2-x}, the most favourable solution site was the neutral tri-vacancy while in UO_{2+x}, it was the uranium vacancy. In UO_2, the most stable solution site was different for different fission products. For example, Xe was most stable at the neutral tri-vacancy but Cs and Rb preferred the uranium vacancy site. Although the predictions for Xe, Cs and Rb in UO_2 are supported by experimental studies (Matzke & Blank 1989) there are no additional data with which to compare our other results.

The model was expanded to consider solution from secondary binary oxide phases such as Cs_2O, BaO, La_2O_3 and ZrO_2. Again, when it was possible to make a comparison, the calculations compared favourably with experimental results. Perhaps the most significant success of the model is that it is able to predict the differences in the variation of solubility with stoichiometry that are exhibited by the different fission product compounds. Eventually we hope that this will lead to an understanding of how, with changing fuel history, the components of the precipitates might change. In this regard, we have demonstrated that the methodology used in the study can be used to investigate reactions between different binary oxide phases. In this case we investigated the stability of perovskite phases $BaZrO_3$, $SrZrO_3$, $BaUO_3$ and $SrUO_3$.

In the last part of the study, we attempted to predict how the charge states of Xe, I, Br and Te might change with fuel stoichiometry. For I, Br and Te, the calculations clearly predict that in UO_{2-x} these species are most stable as anions but that in UO_{2+x} they are cations. As such, these ions will affect the redox characteristics of the fuel.

This work has been funded by the Corporate Research programme of the Atomic Energy Authority at Harwell laboratory.

We thank Dr A. H. Harker and Dr R. G. J. Ball for providing a number of the electron-gas potentials used in this work. Informative discussions with Professor A. M. Stoneham, Dr A. B. Lidiard, Dr J. H. Harding and Dr Hj. Matzke are gratefully acknowledged.

PHILOSOPHICAL TRANSACTIONS OF THE ROYAL SOCIETY A MATHEMATICAL, PHYSICAL & ENGINEERING SCIENCES

Table 6. *Short-range pair potential parameters*

interacting ions	potential parameters			interacting ions	potential parameters		
	A/eV	ρ/Å[a]	C/(eV Å^{-6})		A/eV	ρ/Å	C/(eV Å^{-6})
U^{4+}–U^{4+}	18600.00	0.27468	32.64	I^{-}–U^{4+}	6366.08	0.3389	96.48
U^{4+}–O^{2-}	2494.20	0.34123	40.16	I^{-}–O^{2-}	619.04	0.42657	114.23
O^{2-}–O^{2-}	108.00	0.38000	56.06	I^{0}–U^{4+}	7948.45	0.31427	71.84
Xe^{0}–U^{4+}	6139.16	0.33950	71.84	I^{0}–O^{2-}	465.13	0.44074	108.38
Xe^{0}–O^{2-}	598.00	0.42570	108.38	I^{+}–U^{4+}	6275.23	0.32892	48.62
Xe^{+}–U^{4+}	5190.59	0.33433	48.62	I^{+}–O^{2-}	783.99	0.40251	64.34
Xe^{+}–O^{2-}	1045.00	0.38557	64.34	Br^{-}–U^{4+}	3753.41	0.36346	73.88
Cs^{+}–U^{4+}	18659.60	0.29505	48.62	Br^{-}–O^{2-}	214.03	0.48240	85.24
Cs^{+}–O^{2-}	649.60	0.41421	64.34	Br^{0}–U^{4+}	7271.14	0.30145	50.34
Ba^{2+}–U^{4+}	85887.00	0.25014	42.58	Br^{0}–O^{2-}	523.82	0.41412	55.13
Ba^{2+}–O^{2-}	1565.69	0.36970	41.61	Br^{+}–U^{4+}	6081.46	0.30887	31.80
La^{3+}–U^{4+}	189950.29	0.23162	36.02	Br^{+}–O^{2-}	894.84	0.37649	40.11
La^{3+}–O^{2-}	1638.92	0.35490	33.86	Te^{2-}–U^{4+}	5062.54	0.36536	108.42
Ce^{4+}–U^{4+}	101860.0	0.24076	23.87	Te^{2-}–O^{2-}	286.21	0.48664	123.22
Ce^{4+}–O^{2-}	1984.20	0.3494	26.44	Te^{-}–U^{4+}	5811.18	0.34529	96.48
Kr^{0}–U^{4+}	5912.78	0.31910	50.34	Te^{-}–O^{2-}	504.39	0.43963	114.23
Kr^{0}–O^{2-}	800.38	0.38880	55.13	Te^{0}–U^{4+}	7634.60	0.31549	71.84
Rb^{+}–U^{4+}	13858.09	0.28340	31.80	Te^{0}–O^{2-}	334.19	0.45743	108.38
Rb^{+}–O^{2-}	962.18	0.37723	40.11	Te^{+}–U^{4+}	5572.80	0.33576	48.62
Sr^{2+}–U^{4+}	27942.87	0.23580	21.30	Te^{+}–O^{2-}	640.97	0.41223	64.34
Sr^{2+}–O^{2-}	1696.09	0.34259	25.88	Te^{2+}–U^{4+}	7050.32	0.31133	42.58
Y^{3+}–U^{4+}	29886.18	0.23170	14.28	Te^{2+}–O^{2-}	1201.98	0.36785	41.61
Y^{3+}–O^{2-}	1766.40	0.33849	19.43	I^{-}–I^{-}	1234.18	0.43723	206.99
Zr^{4+}–U^{4+}	31401.90	0.21880	10.20	Cs^{+}–I^{-}	2598.07	0.38219	80.24
Zr^{4+}–O^{2-}	1849.10	0.33270	14.40				

[a] 1 Å = 10^{-10} m.

Appendix A. Parameter selection

(*a*) *Short-range pair potentials*

A consistent set of short-range interactions was calculated using the electron-gas code of Harding & Harker (1982). As a preliminary step, it is necessary to determine the electron densities of component ions embedded in the bulk oxide (the effect of embedding on electron densities has been discussed by Grimes (1990)). In the present study, cation densities were calculated numerically (Herman & Skillman 1963) and incorporated a relativistic correction (Cowan & Griffin 1976). Densities for O, Br, I, Xe, Kr and Te were determined analytically from expansions of Slater functions (Clementi & Roetti 1974) subject to an embedding Madelung potential specific to UO_2. The electron-gas method itself was essentially that due to Wedepohl (1967) with exchange interactions approximated by the Handler relationship (Handler 1974) and correlation effects by the Wigner equations (1938). The electron gas data were used to determine the A and ρ parameters of the Buckingham potentials reported in table 6 through a fitting procedure.

Many-body electron dispersion effects were calculated using the formulae of Slater & Kirkwood (1931) as outlined by Fowler & Pyper (1985). These were incorporated directly into the Buckingham potential form as the C_6 term (see table 6 for details). Since no polarizabilities were available for the open shell charge states of Br, I, Xe

Table 7. *Shell model parameters*

ion	Y (e)	k/(eV Å^{-2})	ion	Y (e)	k/(eV Å^{-2})	ion	Y (e)	k/(eV Å^{-2})
U^{4+}	−6.54	98.24	La^{3+}	−8.3	1449.0	Y^{3+}	−6.9	1427.3
O^{2-}	−4.4	296.8	Ce^{4+}	−7.3	1957.0	Zr^{4+}	−5.9	2030.3
Xe°	−11.3	460.8	Kr°	−9.9	573.7	I^-	−12.3	367.6
Cs^+	−10.3	675.0	Rb^+	−8.9	850.9	Br^-	−10.9	384.9
Ba^{2+}	−9.3	989.2	Sr^{2+}	−7.9	1189.6	Te^{2-}	−13.3	291.3

Table 8. *Experimental and calculated crystal properties for* UO_2

(r_0, lattice constant (Å); E_L, lattice energy (eV); B, bulk modulus (10^{11} dyn cm^{-2})[a]; S_1, shear modulus (10^{11} dyn cm^{-2}); S_2, shear modulus (10^{11} dyn cm^{-2}); P_∞, high frequency polarizability[b]; P_0, zero frequency polarizability.)

crystal properties	reference	experimental	calculated
r_0	Wyckoff (1963)	2.734	2.734
E_L	Benson *et al.* (1963)	106.7	105.56
B	Fritz (1976)	20.89±0.17	27.08
S_1	Fritz (1976)	13.52±0.17	18.33
S_2	Fritz (1976)	5.97±0.03	8.77
P_∞	Schoenes (1980)	1.25	1.23
P_0	Schoenes (1980), Hampton *et al.* (1987)	6.52	8.71

[a] $B = \frac{1}{3}(C_{11}+2C_{12})$, $S_1 = \frac{1}{2}(C_{11}-C_{12})$ and $S_2 = C_{44}$, where C_{11}, C_{12}, and C_{44} are elastic constants.
[b] $P_\infty = (1-\epsilon_\infty^{-1})^{-1}$ and $P_0 = (\epsilon_\infty^{-1}-\epsilon_0^{-1})^{-1}$, where ϵ_∞ and ϵ_0 are dielectric constants at zero and high frequency.

and Te, the C_6 terms were assumed to be well matched by the equivalently charged alkali and alkaline earth ions of nearest atomic number (i.e. Cs^+ potentials for Xe^+, Ba^{2+} for Xe^{2+}, etc.). The uncertainty introduced by the use of such an approximation is small.

It should be noted that when the electron gas potentials were used to calculate perfect lattice parameters for UO_2, there was a residual bulk lattice strain of 3.5%. Although this is small, it was decided to remove it by making the lattice oxygen–oxygen potential slightly more attractive. Apart from this small alteration, no other change to the electron gas potentials was necessary. The consistency that this provides is an important feature of our model.

(*b*) *Shell model parameters*

Values of Y and k specific to each ion were chosen so that the free-ion polarizability, α, is given by (Cochran 1973): $\alpha = Y^2/k$. Values for O^{2-} and U^{4+} are exceptions to this procedure as they were empirically fitted to yield good dielectric constants for UO_2. The importance of this is discussed below.

(*c*) *Reliability of parameters*

One way of determining the reliability of a potential model is to calculate perfect lattice properties. The results of table 8 show that the model is successful in calculating lattice properties for UO_2. The properties described in table 8 are

Table 9. *Lattice energies of fission product precipitates (negative electronvolts)*

	previous estimates[a]	calculated[b]
Cs_2O	—	21.24
Rb_2O	22.42	22.07
BaO	31.39	31.73
SrO	33.34	34.01
La_2O_3	129.05	130.59
Y_2O_3	131.67	135.52
CeO_2	99.77	106.30
ZrO_2	115.95	113.78
CsI	6.22	5.93

[a] CRC Handbook of Chemistry and Physics.
[b] Lattice energies are fully minimized to zero strain and refer to separated ions at rest at infinity.

physically significant for defect calculations. Success in reproducing moduli means that lattice ion relaxation for small displacements from equilibrium will be well modelled. Accurate polarizabilities mean that long-range polarization energies can be reproduced.

The electron-gas potentials for the fission product ions were used to calculate the lattice energies of the appropriate binary oxides (table 9). The agreement with previous estimates is good.

The electron-gas lattice–lattice potentials used in this study are inferior in their representation of bulk lattice properties to those derived previously using purely empirical fitting procedures (Catlow 1977; Jackson & Catlow 1986). However, previous studies have found that mixing empirical and electron-gas potentials can lead to spurious results. Thus, since there were no structural data on which to base empirical fitting of fission product-lattice potentials, it was necessary to use electron-gas methodology to derive a fully consistent set of fission product–lattice and lattice–lattice potentials.

Comparing calculated and experimental perfect lattice properties is only relevant to small displacements around equilibrium lattice positions (Harding 1989). In defect calculations displacements are often much greater. It is possible to justify the use of a potential for modelling large ionic displacements if comparison can be made with predictions from other models or to experimental results. A discussion of experimental results is found in the main text. A detailed comparison of results from Mott–Littleton and embedded quantum cluster simulations can be found in the literature (Grimes 1988; Grimes *et al.* 1989*a–c*). This includes comparison of solution energies for inert gas atoms trapped at uranium vacancy sites (Grimes 1988; Grimes *et al.* 1989*a*). The similarity of values obtained from both models increases our confidence in the potential model.

Appendix B. Equilibrium trap formation energies

The energy required to form a trap site will depend on the stoichiometry of the lattice. Since the intrinsic disorder in UO_2 is of the oxygen Frenkel type, with a minority concentration of Schottky defects, the defect equilibria controlling the formation of the trap sites are (in Kröger–Vink notation):

Table 10. *Effective energy to form trap sites*[a]

(Schottky trio formation energy, $E_s = 13.34$ eV; oxygen Frenkel pair formation energy, $E_f = 6.82$ eV; binding energy of a di-vacancy, $B_{DV} = 3.24$ eV; binding energy of a neutral tri-vacancy, $B_{NTV} = 4.93$ eV; binding energy of a charged tetra-vacancy, $B_{CTV} = 8.89$ eV.)

	UO_{2-x}		UO_2		UO_{2+x}	
trap site	formation expression	formation energy/eV	formation expression	formation energy/eV	formation expression	formation energy/eV
oxygen vacancy	nil	0.00	$\frac{1}{2}E_f$	3.41	E_f	6.82
uranium vacancy	E_s	13.34	$E_s - E_f$	6.51	$E_s - 2E_f$	−0.31
di-vacancy	$E_s - B_{DV}$	10.09	$E_s - \frac{1}{2}E_f - B_{DV}$	6.68	$E_s - E_f - B_{DV}$	3.27
neutral tri-vacancy	$E_s - B_{NTV}$	8.41	$E_s - B_{NTV}$	8.41	$E_s - B_{NTV}$	8.41
charged tetra-vacancy	$2E_s - B_{CTV}$	17.78	$2E_s - E_f - B_{CTV}$	10.96	$2E_s - 2E_f - B_{CTV}$	4.13

[a] The formation energy of an interstitial site is zero for all stoichiometries.

(i) oxygen Frenkel formation

$$O_O^\times \longleftrightarrow O_i'' + V_O^{\cdot\cdot}$$

for which the equilibrium constant, K_f, is given by

$$K_f = [O_i''][V_O^{\cdot\cdot}] = 2\exp(S_f/k_B)\exp(-E_f/k_B T)$$

(assuming concentrations refer to mol fractions);

(ii) Schottky trio formation

$$2O_O^\times + U_U^\times \longleftrightarrow 2V_O^{\cdot\cdot} + V_U'''' + 2O_O^\times + U_U^\times$$

with the equilibrium constant, K_s, given by

$$K_s = [V_U''''][V_O^{\cdot\cdot}]^2 = 4\exp(S_s/k_B)\exp(-E_s/k_B T).$$

As discussed in previous articles (see, for example, Catlow 1978; Ball & Grimes 1990), the formation energy of the trap site, E_T, can be related to the Frenkel (E_f) and Schottky (E_s) energies and to the defect cluster binding energies, B_{DV}, B_{NTV} and B_{CTV}. The appropriate expressions and calculated values are given in table 10. Variation of formation energy with stoichiometry is essentially a consequence of the different roles that Frenkel defects play in maintaining a constant stoichiometry. For example, formation of a uranium vacancy in UO_{2-x} is accompanied by the formation of two oxygen vacancies. This is simply the Schottky equilibrium so that, $E_T = E_s$. However, in UO_2, the equilibrium between interstitial oxygen and oxygen vacancies means that uranium vacancy formation proceeds via,

$$O_i'' + O_O^\times + U_U^\times \longleftrightarrow V_U'''' + V_O^{\cdot\cdot} + 2O_O^\times + U_U^\times$$

and the equilibrium constant K_U is given by,

$$K_U = \frac{[V_U''''][V_O^{\cdot\cdot}]}{[O_i'']} = \frac{[V_U''''][V_O^{\cdot\cdot}]^2}{[O_i''][V_O^{\cdot\cdot}]} = \frac{K_s}{K_f}$$

so that, $E_T = E_s - E_f$.

Lastly, in UO_{2+x}, we can write

$$2O_i'' + U_U^\times \longleftrightarrow V_U'''' + 2O_O^\times + U_U^\times,$$

which leads to the relationship $E_T = E_s - 2E_f$.

The formation energies reported in table 10 suggest that in UO_{2-x} the minority vacancy defect concentration will be dominated by the neutral tri-vacancy (the majority defect is of course the oxygen vacancy). In UO_2, both the uranium vacancy and the di-vacancy cluster are the important minority defects with the uranium vacancy becoming the most populous minority defect in UO_{2+x}.

References

Adamson, M. G., Aitken, E. A. & Vaidyanathen, S. 1982 *Nature* **295**, 49.

Ball, R. G. J. & Grimes, R. W. 1990 *J. chem. Soc. Faraday Trans.* **86**, 1257.

Ball, R. G. J., Burns, W. G., Henshaw, J., Mignanelli, M. A. & Potter, P. E. 1989 *J. nucl. Mater.* **167**, 191.

Bates, J. L., Hinman, C. A. & Kawada, T. 1967 *J. Am. Ceram. Soc.* **50**, 652.

Benson, G. C., Freeman, P. I. & Dempsey, E. 1963 *J. Am. Ceram. Soc.* **46**, 43.

Catlow, C. R. A. 1977*a* *Proc. R. Soc. Lond.* A **353**, 533.

Catlow, C. R. A. 1977*b* *J. chem. Soc. Faraday Trans.* **74**, 1901.

Catlow, C. R. A. 1978 *Proc. R. Soc. Lond.* A **364**, 473.

Catlow, C. R. A. & Fender, B. E. F. 1975 *J. Phys.* C **8**, 3267.

Catlow, C. R. A. & James, R. 1982 *Proc. R. Soc. Lond.* A **384**, 157.

Catlow, C. R. A. & Mackrodt, W. C. 1982 In *Computer simulation of solids* (ed. C. R. A. Catlow & W. C. Mackrodt). Berlin: Springer-Verlag.

Clementi, E. & Roetti, C. 1974 *Atomic Nucl. Data Tables* **14**, no. 3–4.

Cochran, W. 1973 *The dynamics of atoms in crystals*, p. 55. London: Arnold.

Collins, D. R. & Catlow, C. R. A. 1900 Submitted to *Am. Min.*

Cowan, R. D. & Griffin, D. C. 1976 *J. opt. Soc. Am.* **66**, 1010.

CRC Handbook of Chemistry and Physics 1984 D101 (ed. R. C. Weast). CRC Press, Boca Raton, 65th edn.

Cubicciotti, D. 1988 *J. Nucl. Mater.* **154**, 53.

Davies, J. H. & Ewart, F. T. 1971 *J. nucl. Mater.* **41**, 143.

De Alleluia, I. B., Hoshi, M., Jocher, W. G. & Keller, C. 1981 *J. inorg. nucl. Chem.* **43**, 1831.

Dick, B. G. & Overhauser, A. W. 1958 *Phys. Rev.* **112**, 90.

Ewart, F. T., Taylor, R. G., Horspool, J. M. & James, G. 1976 *J. nucl. Mater.* **61**, 254.

Fee, D. C. & Johnson, C. E. 1978 *J. inorg. nucl. Chem.* **40**, 1375.

Fee, D. C., Kim, K. Y. & Johnson, C. E. 1979 *J. inorg. nucl. Chem.* **84**, 286.

Fowler, P. W., Knowles, P. J. & Pyper, N. C. 1985 *Molec. Phys.* **56**, 83.

Fritz, I. J. 1976 *J. appl. Phys.* **47**, 4353.

Gittus, J. H., Matthews, J. R. & Potter, P. E. 1989 *J. nucl. Mater.* **166**, 132.

Grimes, R. W. 1988 UKAEA Rep. AERE-TP. 1308.

Grimes, R. W. 1990 *Mol. Sim.* **5**, 9.

Grimes, R. W. & Catlow, C. R. A. 1990 *J. Am. Ceram. Soc.* **73**, 3251.

Grimes, R. W., Catlow, C. R. A. & Stoneham, A. M. 1989*a* *J. Phys. Condens. Matter* **1**, 7367.

Grimes, R. W., Catlow, C. R. A. & Stoneham, A. M. 1989*b* *J. chem. Soc. Faraday Trans.* **85**, 485.

Grimes, R. W., Catlow, C. R. A. & Stoneham, A. M. 1989*c* *J. Am. Ceram. Soc.* **72**, 1856.

Hampton, R. N., Saunders, G. A., Harding, J. H. & Stoneham, A. M. 1987 *J. nucl. Mater.* **150**, 17.

Handler, G. S. 1974 *J. chem. Phys.* **61**, 4824.

Harding, J. H. 1989 *Cryst. Latt. Def. amorph. Mater.* **18**, 247.

Harding, J. H. & Harker, A. H. 1982 UKAEA Rep. AERE-R. 10425.

Harding, J. H., Masri, P. & Stoneham, A. M. 1980 *J. nucl. Mater.* **92**, 73.

Herman, F. & Skillman, S. 1963 *Atomic structure calculations.* New Jersey: Prentice-Hall.

Imoto, S. 1986 *J. nucl. Mat.* **140**, 19.

Jackson, R. A. & Catlow, C. R. A. 1985*a* *J. nucl. Mater.* **127**, 161.

Jackson, R. A. & Catlow, C. R. A. 1985*b* *J. nucl. Mater.* **127**, 167.
Jackson, R. A. & Catlow, C. R. A. 1988 *Mol. Sim.* **1**, 207.
Jackson, R. A., Murray, A. D., Harding, J. H. & Catlow, C. R. A. 1986 *Phil. Mag.* A **53**, 27.
Kleykamp, H. 1979 *J. nucl. Mater.* **84**, 109.
Kleykamp, H. 1985 *J. nucl. Mater.* **131**, 221.
Kleykamp, H. 1990 *J. nucl. Mater.* **171**, 181.
Kleykamp, H., Paschoal, J. O., Pejsa, R. & Thommler, F. 1985 *J. nucl. Mater.* **130**, 426.
Kovba, L. M. 1970 *Dokl. Chem.* (*Engl. Trans.*) **194**, 632.
Latta, R. E. & Fryxell, R. E. 1970 *J. nucl. Mater.* **35**, 195.
Leslie, M. 1982 Program CASCADE documentation, SERC Daresbury Laboratory Report, DL/SCI/TM31T.
MacInnes, D. A. & Winter, P. W. 1988 *J. Phys. Chem. Solids* **49**, 143.
Maeda, A., Ohmichi, T., Fukushima, S. & Handa, M. 1984 *J. nucl. Sci. Tech.* **21**, 800.
Markin, T. L., Street, R. S. & Crouch, E. C. 1970 *J. inorg. nucl. Chem.* **32**, 59.
Matzke, Hj. 1980 *Rad. Effects* **53**, 219.
Matzke, Hj. 1987 *J. chem. Soc. Faraday Trans.* **83**, 1121.
Matzke, Hj. 1989 *Ann. Chim. Fr.* **14**, 133.
Matzke, Hj. & Blank, H. 1989 *J. nucl. Mater.* **166**, 120.
Matzke, Hj. & Davies, J. A. 1967 *J. appl. Phys.* **38**, 805.
Moore, C. E. 1971 'Analysis of optical spectra'. NSRDS-NBS 34, Office of Standard Reference Data, National Bureau of Standards, Washington, D.C.
Mott, N. F. & Littleton, M. J. 1938 *Trans. Faraday Soc.* **34**, 485.
Nichols, F. A. 1979 *J. nucl. Mater.* **84**, 1.
Norgett, M. J. 1974 UKAEA Rep. AERE-R. 7650.
Norgett, M. J. & Fletcher, R. 1970 *J. Phys.* C **3**, L190.
Phillips, J. R., Waterbury, G. R. & Vanderborgh, N. E. 1974 *J. inorg. nucl. Chem.* **36**, 17.
Pearce, J. H., Sumerling, R. & Hargreaves, R. 1983 *J. nucl. Mater.* **116**, 1.
Potter, P. E. 1988 *Pure appl. Chem.* **60**, 323.
Prussin, S. G., Olander, D. R., Lau, W. K. & Hansson, L. 1988 *J. nucl. Mater.* **154**, 25.
Pulham, R. J. & Richards, M. W. 1990 *J. nucl. Mater.* **171**, 319.
Pyper, N. C. & Grant, I. P. 1978 *J. chem. Soc. Faraday Trans.* **74**, 1885.
Romberger, K. A., Baes, C. F. & Stone, H. H. 1967 *J. inorg. nucl. Chem.* **29**, 1619.
Sari, C., Walker, C. T. & Schumacher, G. 1979 *J. nucl. Mater.* **79**, 255.
Schoenes, J. 1980 *Phys. Rep.* **63**, 301.
Schuster, I. & Lemaignan, C. 1989 *J. nucl. Mater.* **166**, 348.
Shannon, R. D. 1976 *Acta Crystallogr.* A **32**, 751.
Stater, J. C. & Kirkwood, J. G. 1931 *Phys. Rev.* **37**, 682.
Templier, C., Garem, H. & Riviere, J. P. 1986 *Phil. Mag.* A **53**, 667.
Thomas, L. E. & Guenther, R. J. 1989 *Mat. Res. Soc. Symp. Proc.* **127**, 293.
Thomas, L. E., Einziger, R. E. & Woodley, R. E. 1989 *J. nucl. Mater.* **166**, 243.
Tomlinson, S. M., Catlow, C. R. A. & Harding, J. H. 1990 *J. Phys. Chem. Solids* **51**, 477.
Turnbull, J. A. & Cornell, R. M. 1971 *J. nucl. Mater.* **41**, 156.
Une, K. 1985 *J. nucl. Sci. Tech.* **22**, 586.
Walker, C. T. 1978 *J. nucl. Mater.* **74**, 358.
Wedepohl, P. T. 1967 *Proc. phys. Soc.* **92**, 79.
Willis, B. T. M. 1964 *Proc. Br. Ceram. Soc.* **1**, 9.
Wyckoff, R. W. G. 1963 *Crystal structures*, vol. 1, 2nd edn, p. 243. New York: Interscience.
Yang, T.-T. & Tsai, C.-H. 1989 *J. nucl. Mater.* **166**, 252.

Received 30 January 1991; accepted 20 February 1991

PHILOSOPHICAL TRANSACTIONS OF THE ROYAL SOCIETY A MATHEMATICAL, PHYSICAL & ENGINEERING SCIENCES